Chapter 2

Experimental and instrumentations

2.1 Experimental

In the present work, we have prepared nickel ferrite, $NiFe_2O_4$ (NFO) and Cobalt substituted nickel ferrite by a facile sol-gel method. MOF materials can be synthesised by various synthesis routes like hydro/ solvothermal technique, microwave, electrochemical and mechanochemical etc. [81] but here we adopted a facile precipitation method for the synthesis of Co-MOF, Ni-Fe PBA nanocube and ZnDTO MOF. After that, MOFs were modified through a different strategy such as the formation of hollow cubes with the treatment of ammonia solution of Ni-Fe PBA, formation of porous oxide cubes by annealing the Ni-Fe PBA in air, synthesis of N/S/Zn doped porous carbon by carbonization of ZnDTO MOF in an inert atmosphere and nanocomposite formation with Co_3O_4 and N/S/Zn doped porous carbon.

2.1.1 Materials

Nickel nitrate hexahydrate [$Ni(NO_3)_2.6H_2O$], Iron nitrate nonahydrate [$Fe(NO_3)_3{\cdot}9H_2O$] and ammonia (25%) were purchased from Fisher Scientific, Mumbai, India and Citric acid ($C_6H_8O_7$) was purchased from SRL, Mumbai, India. Anthranilic acid ($C_7H_7NO_2$), Cobalt nitrate hexahydrate $Co(NO_3)_2.6H_2O$**,** Sodium hydroxide pellets (NaOH), Pottasium hydroxide pellets (KOH), N-methyl pyrrolidone (NMP), potassium ferricyanide [$K_3Fe(CN)_6$], Dithiooxamide ($C_2H_4N_2S_2$), Zinc acetate dihydrate ($C_4H_6O_4Zn.2H_2O$) were bought from Sigma Aldrich, India. Polyvinyl pyrrolidone (PVP), Sodium dodecyl sulphate (SDS), Cobalt chloride hexahydrate ($CoCl_2{\cdot}6H_2O$) and Sodium borohydride ($NaBH_4$) were bought from Himedia, India. Deionized water (DI) (pH=7.0, resistivity=18.0 MΩ) was used to prepare all the aqueous solutions and Nafion perfluorinated resin solution (5 wt. % in water) (Sigma Aldrich, India) used as a binder during the fabrication of commercial GCE.

2.1.2 Synthesis of nickel ferrite and cobalt-substituted nickel ferrite

Nickel ferrite ($NiFe_2O_4$) and Co-substituted Nickel ferrite i.e $M_xNi_{1-x}Fe_2O_4$ (M = Co and x = 0.25, 0.5, 0.75, and 1) were prepared with a conventional citric acid-assisted sol-gel method as follows: 0.01 mol (2.90 g) of $Ni(NO_3)_2.6H_2O$ was added into 100 mL of H_2O (Milli Q) followed by addition of 0.02 mol (8.07 g) of $Fe(NO_3)_3 \cdot 9H_2O$ (molar ratio of Ni/Fe = 1/2), and 0.03 mol (5.76 g) of citric acid ($C_6H_8O_7$) dissolved in 100 mL of H_2O was added to the above solution with constant stirring with the help of a Teflon-lined magnetic pellet. During this time the pH of the reaction mixture was adjusted to 7 by adding ammonia solution. After constant stirring of the whole mixture for three hours it was heated to around 70 °C to remove excess water until the mixture produced metal ion-rich sol followed by the gel. This removal of excess water produced a viscous gel, and the continuous heating initiated self-combustion of the reaction mixture, and a finally foamy nickel ferrite was formed.

The prepared sample was milled uniformly in an agate mortar followed by annealing at 600 °C, 700 °C, 800 °C, 900 °C for three hours at a heating rate of 10 °C min^{-1} in N_2 atmosphere to obtain pure and crystalline $NiFe_2O_4$ powders. After cooling, the sample was again ground into a fine powder for electrochemical measurements. A similar procedure was adopted for the preparation of Ni- and Co-substituted ferrite substituted $M_xNi_{1-x}Fe_2O_4$ (M = Co; $0 < x < 1$; 0.5 and 1). The synthesis of the spinel catalysts is shown in Figure 2.1.

2.1.2.1 Electrode Preparation

Spinel materials electrodes were made by drop-casting the 10 µL ink of catalysts onto the surface of the glassy carbon electrode (GCE) (geometric area 0.07 cm^2). Spinel catalysts were dispersed in a solvent consisting of water, ethanol, and Nafion (5 wt % in water) followed by sonicated for two hours to form a 10 mg/mL homogeneous ink. The volume

ratio of water: ethanol: Nafion was kept at 1:4:0.05. Prior to drop-casting, the GCE was cleaned properly on a polishing cloth using 0.03 µM alumina powder for 15 minutes followed by sonication in ethanol and water and finally dried at room temperature.

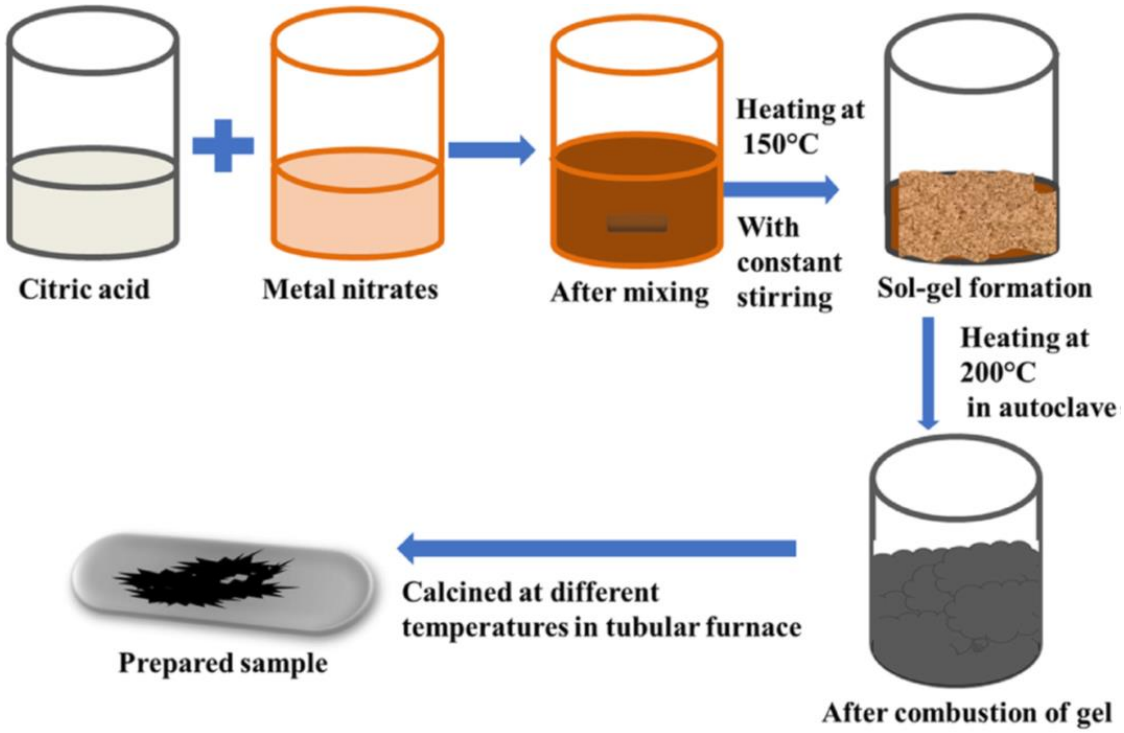

Figure 2.1 Schematic pathways for the preparation of the spinel catalysts.

2.1.3 Synthesis of Co-MOF

A facile and straightforward precipitation procedure is adopted to synthesise Co-MOF. For this, we took the two mmol of Anthranilic acid (AA) in one beaker in 10 mL of ethanol and sonicated it to dissolve. Then added 200 µL of five mmol of NaOH in it. In another beaker, prepare the solution of one mmol of cobalt nitrate hexahydrate in 10 mL DI water and add dropwise into the above mixture under stirring at 600 rpm and heating (@90 ℃). Then leave the reaction undisturbed for four hours. After that, the precipitates are collected by centrifugation, washed with water many times, and dried in a vacuum oven at 60 ℃. The reaction mechanism of the synthesis of Co-MOF is shown in Figure 2.2.

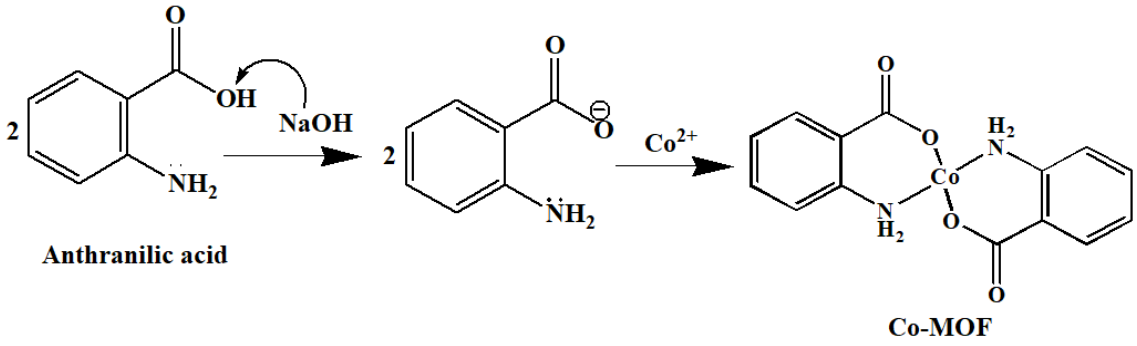

Figure 2.2 Reaction mechanism for the synthesis of Co-MOF.

2.1.3.1 Electrode preparation

For the electrode fabrication, firstly, the ink was prepared by the dispersion of 6 mg of the catalyst into 1mL of NMP and 5 µL of Nafion (as a binder) and ultrasonicated for two hours. Then an aliquot of 10 µL of the homogenised catalyst ink was drop cast onto the cleaned surface of GCE (geometric area=0.07 cm^2) by micropipette, dried in a vacuum oven at 60 ℃ for 4 to 5 hours, and then used for electrochemical measurements.

2.1.4 Synthesis of ZnDTO framework and nanocomposite of Co_3O_4 and N/S doped porous carbon

2.1.4.1 Synthesis of ZnDTO framework

The ZnDTO metal-organic framework is synthesized by a simple and facile precipitation method [85]. In this method, 2.07 mmol of DTO (dissolved in 50 mL DMF) was added slowly to the solution mixture of 2.07 mmol of Zinc acetate and 0.5 g of PVP dissolved in 50 mL of DMF under constant stirring and heating at 80 °C. Then this solution mixture was kept under the same reaction condition for 1 hour. Next, yellow-coloured ZnDTO precipitates were collected and washed thoroughly with DI water and ethanol. Finally, the collected material was vacuum dried at 50 °C for 12 hours and preserved for further experimentations.

2.1.4.2 Synthesis of N/S/Zn doped porous carbon (NSC)

NSC was synthesized by carbonizing 100 mg of ZnDTO in a tubular furnace under an

inert atmosphere. Three different samples were prepared by heating ZnDTO at three different temperatures (500 °C, 700 °C and 900 °C) for 3 hours, and the temperatures were chosen based on TGA data. Thus, as-resultant carbonized products were designated as NSC-5, NSC-7 and NSC-9 on the basis of selected carbonization temperatures of 500 °C, 700 °C and 900 °C, respectively.

Similarly, to compare the contribution of Zn metal in a dual-doped carbon matrix, the optimized sample, NSC-7 (as discussed later in the electrochemical section), is treated with acid. For this purpose, 50 mg of NSC-7 was kept in 25 mL of 2 M HCl solution at room temperature under constant stirring at 600 rpm for 5 hours. After that, it is centrifuged, washed with DI water, and vacuum dried at 60 °C in the oven. The as-washed material thus obtained is designated as NSC-7AW.

The synthesis method of the ZnDTO framework, their carbonization and acid treatment are presented in Figure 2.3.

2.1.4.3 Hydrothermal synthesis of Co_3O_4 nanoparticles

Co_3O_4 nanoparticles are synthesized by a hydrothermal synthesis process [113]. Herein, first of all, 1.0 mmol SDS and 1.0 mmol $CoCl_2 \cdot 6H_2O$ were dissolved in 20 mL DI water under vigorous stirring @ 1000 rpm at room temperature to get a clear pink solution. After that, the pink solution was reduced by gradually adding 0.5 mmol $NaBH_4$ under vigorous stirring. With the addition of $NaBH_4$, the pink micellar solution turns instantly black. Finally, the reaction mixture was given hydrothermal treatment at 160 °C for 15 hours. After the reaction was completed, the black product was collected and washed with DI water and absolute ethanol and then dried in a vacuum oven at 60 °C.

2.1.4.4 Synthesis of nanocomposites

In order to enhance the electrochemical performance of the NSC-7, a nanocomposite

material is formed by the physical mixing of Co_3O_4 nanoparticles with NSC-7. For this, 5 mg Co_3O_4 nanoparticles were dispersed in 7 mL ethanol with the help of ultrasonication for 30 minutes, and then 3 mg NSC-7 was added to this dispersion. Finally, the mixture

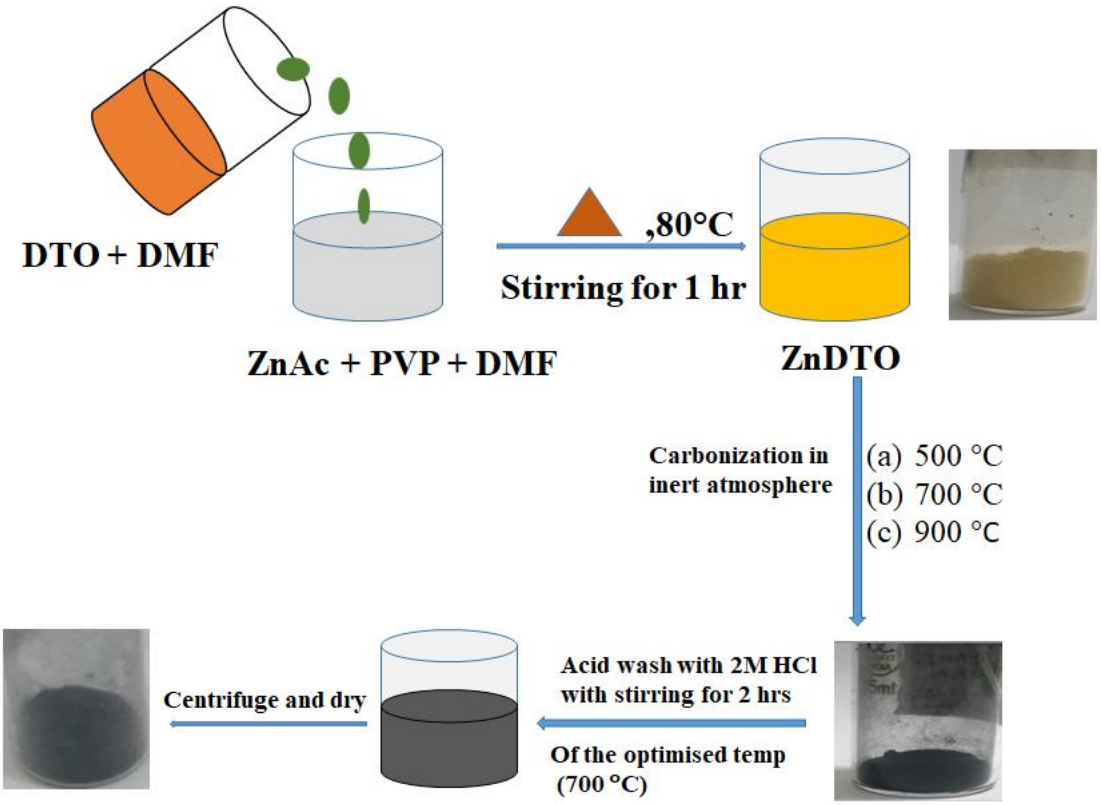

Figure 2.3 Schematic of the synthesis of ZnDTO and NSCs.

of both dispersions was subjected to stirring at 600 rpm for 10 hours to ensure complete mixing. After that, nanocomposite material was collected by centrifugation and dried at 60 °C. This nanocomposite is designated as Co_3O_4|NSC-7. A similar procedure was also followed to synthesise the nanocomposite using NSC-7AW and designated as Co_3O_4|NSC-7AW.

2.1.4.5 Electrode fabrication

10 µL catalysts (1mg/mL homogeneous ink) of each kind were drop-casted onto the cleaned surface of GCE (geometric area=0.07 cm^2) to fabricate the working electrodes.

The ink was prepared by dispersion of catalysts in a solvent mixture of water, ethanol, and Nafion (volume ratio is 1:4:0.05) through ultra-sonication for two hours. Finally, as-fabricated electrodes were dried at room temperature and preserved for electrochemical measurements.

2.1.5 Synthesis of NiFe-PBA nanocube and their conversion into hollow cubes and mixed oxides

2.1.5.1 Synthesis of NiFe-PBA nanocubes

NiFe-PBA-NC was prepared by previously reported literature procedure as shown in Figure 2.4 [114]. In this, 0.6 mmol of nickel nitrate and 0.9 mmol of sodium citrate were dissolved in 20 mL of deionized (DI) water to form solution A, and 0.4 mmol of potassium ferricyanide was dissolved in 20 mL of DI water to form solution B. Then, solution B was added to solution A dropwise under stirring (@550 rpm) for 5 min and aged for 7 days. After that precipitate was collected, centrifuged and washed with ethanol and water then dried in the oven at 60 °C.

2.1.5.2 Synthesis of NiFe-PBA nanocage and NiFe oxide

For the synthesis of NiFe-PBA nanocage, 5 mg of NiFe-PBA nanocubes was dissolved in 2.5 mL ethanol and stirred for 1 hour then 2.6 mL of diluted ammonia solution (prepared by adding 5 mL of 25% $NH_3.H_2O$ solution into 15 mL water) was added dropwise and stirred for 2 hours at 550 rpm. As the reaction stopped, it was centrifuged to collect precipitate and dried at 60 °C in the oven. NiFe oxide (porous oxide cube) is formed by annealing the NiFe-PBA-NC at 350 °C for 3 hours with a heating temperature rate of 2 °C min^{-1}.

2.1.5.3 Electrode preparation

The working electrodes are prepared by drop-casting 10 μL ink of catalysts onto the surface of glassy carbon electrodes (GCEs) (geometric area 0.07). Catalysts are dispersed

in a solvent consisting of water, ethanol, and Nafion (5 wt % in water) in the volume ratios of 1:4:0.05 and sonicated for two hours to form a 1mg/mL homogeneous ink.

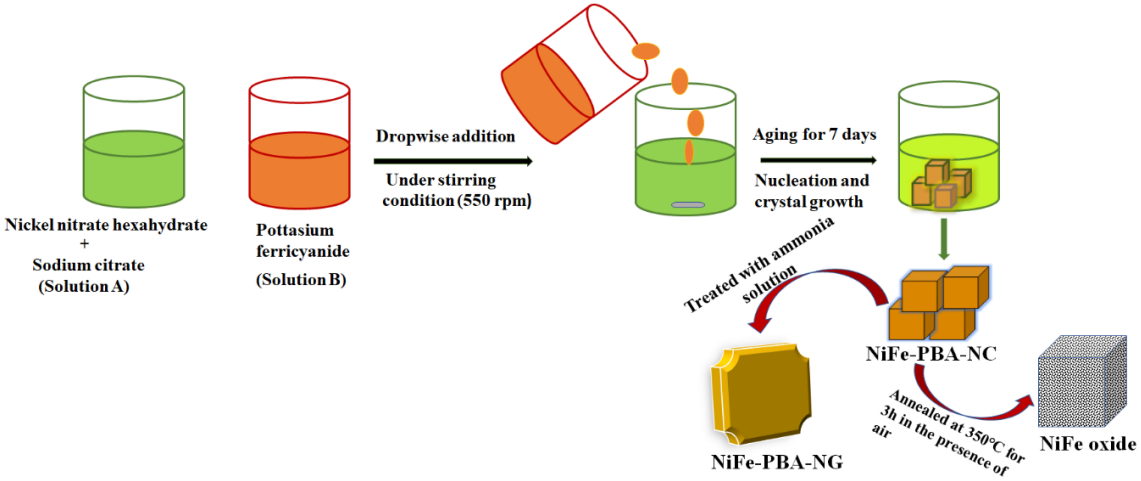

Figure 2.4 Schematic of the synthesis of the Ni-Fe-PBA-NC and transformation into nanocage and oxide.

2.2 Characterizations Techniques

To characterize the synthesized materials, different instrumental tools are used like UV-Vis (UV-Visible spectroscopy), FTIR (Fourier Transform Infrared Spectroscopy), X-ray Diffractometer (XRD), Scanning Electron Microscope (SEM), Energy Dispersive Spectroscopy (EDX), and X-ray Photoelectron Spectroscopy (XPS). TGA is used to find the thermal properties of the as-synthesized material and BET surface area analyzer (BEL Japan) is employed to analyse the surface properties of the samples. Wettability and water contact angles were evaluated with a Contact angle, Apex instrument. For electrochemical measurements, LSV (Linear sweep voltammetry), CV (cyclic voltammetry) and EIS (electrochemical impedance spectroscopy) techniques have been used. A brief background of every technique is discussed in detail.

2.2.1 Structural Characterizations

2.2.1.1 UV-Vis. absorption spectroscopy

UV-Vis. spectroscopy is an important tool for locating the absorbance or reflectance band of any molecule. In this monochromatic UV or visible light pass through the sample and

a graph of light absorbed versus wavelength is obtained. Figure 2.5 shows the UV-Vis. spectrophotometer and its schematic representation.

Lambert-Beer's law states the working principle of the UV-Vis. spectrophotometer. According to this, the concentration of the absorbing species in the solution and the path length are directly related to the absorbance of a solution. This law can be expressed as-

$$log_{10}\frac{I_0}{I} = A = \varepsilon cl \qquad \text{(Eq. 2.1)}$$

Where I_0 is the incident intensity, I is the transmitted intensity of the light, A is absorbance, Ɛ is a constant, designated as the absorptivity or extinction coefficient, c is the concentration of the absorbing species and l is the path length through the sample.

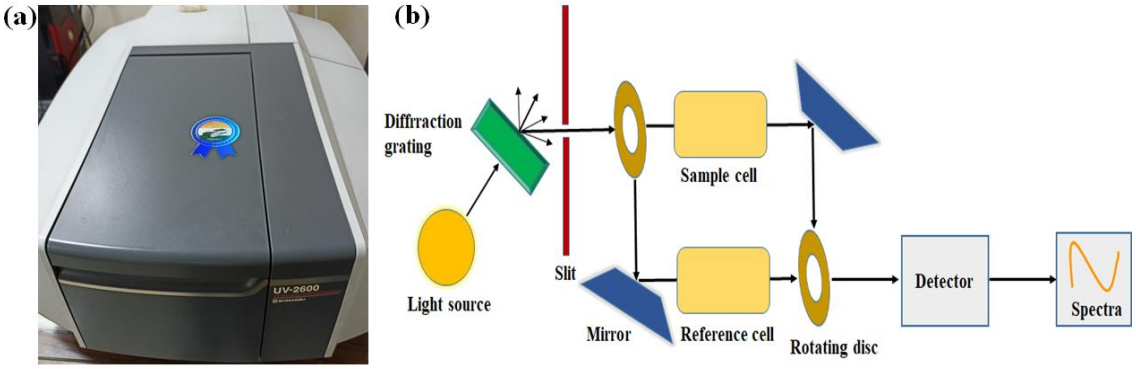

Figure 2.5 (a) Photograph of the UV-Vis. spectrophotometer and (b) schematic representation of the double-beam spectrophotometer.

2.2.1.2 Fourier transform infrared spectroscopy (FT-IR)

To get the infrared spectrum of solid, liquid, or gaseous materials as absorption or emission FT-IR technique is used. By recording the spectrum of material between 4000 and 400 cm^{-1}, various functional groups that are present can be recognised. In this technique, the raw data (interferogram) is transformed mathematically into the actual spectrum via a process known as the Fourier transform. Functional groups in the molecule act as dipole moments corresponding to a specific vibrational energy. When molecules

are exposed to the individual wavelength in the 4000-400 cm^{-1} range, they absorb only those having the energy essential to cause a definite vibration and transmit some other frequencies. Every functional group has a unique set of atoms and bond strength, and since the vibrational energy depends on two parameters, reduced mass (μ) and bond spring constant (k) therefore, vibrations are unique to functional groups, and classes of functional groups. As functional groups bound to the surface of the nanomaterial exhibit distinct FT-IR patterns than free groups, FT-IR can also reveal information about the surface chemistry of nanomaterials. We use 6700- FT-IR, Thermo Scientific Nicolet spectrometer in the spectral range of 450-4000 cm^{-1}.

The most important component of FT-IR spectroscopy is the Michelson interferometer and it is very different from typical infrared dispersive spectroscopy [115]. In the dispersive IR spectroscopy, a sequence of the monochromatic lights is fall on the sample covering a range of the infrared wavelength. Whereas, in the non-dispersive FT-IR spectroscopy, many frequencies of IR light is put on the sample at once using an interferometer and post-processing of the transmitted light.

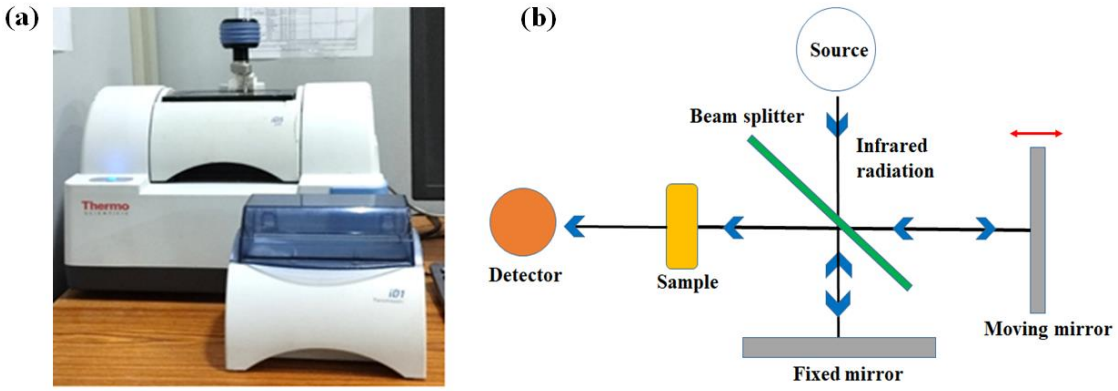

Figure 2.6 (a) Photograph of the FT-IR spectrometer and (b) working principle of the Michelson interferometer.

In the Michelson interferometer, a beam source of diverse IR wavelengths is sent via a beam splitter [Figure 2.6(b)], where half of the wavelengths strike a fixed mirror and the

other half reaches a moving mirror (moves with a constant velocity). Through reflection and recombination (with a path difference between the beams), an interference pattern is created, which is produced as a pattern of the constructive and destructive interference of the recombination. The transmitted portion of the interferogram is then transferred to a detector as the interference pattern (also known as an interferogram) passes through the sample. In order to obtain the whole spectrum in terms of % transmittance vs. wavenumber, the spectrum is compared to a reference sample and the Fourier transform is used.

2.2.1.3 X-ray Powder Diffraction (XRD)

XRD is a highly helpful technique to obtain detailed information about the chemical composition and crystallographic structure of the natural and synthesised materials. Monochromatic X-rays and a crystalline sample constructively interfere to produce the XRD pattern. The sample is exposed to intense monochromatic X-ray radiation, which interacts with the sample in accordance with Bragg's Law ($n\lambda=2d \sin\theta$), resulting in constructive interference and a diffracted ray. The relationship between the X-ray wavelength (λ), diffraction angle (θ) and the lattice spacing (d) in a crystalline sample is given by Bragg's law. All possible lattice diffraction orientations can be accomplished by scanning the sample over a range of 2θ angles and passing the diffracted X-rays from the sample through the detectors. Then, a set of specific d-spacing is created for each sample based on these diffraction peaks (patterns). We then determine the phase and crystallographic structure of the material by comparing the d-spacing with a standard reference pattern.

The prepared samples were characterized by using Rigaku Miniflex 600 X-ray Diffractometer using Cu-Kα (λ=1.5405Å) [Figure 2.7(a)]. The diffractometer was calibrated using silicon powder. Single-crystal silicon was used as a standard for

obtaining the accurate value of 2θ for the calculation of the quasi lattice parameter. The XRD patterns were collected over 10°-80° in 2θ using a step size of 3°/min (these parameters were also varied as per need).

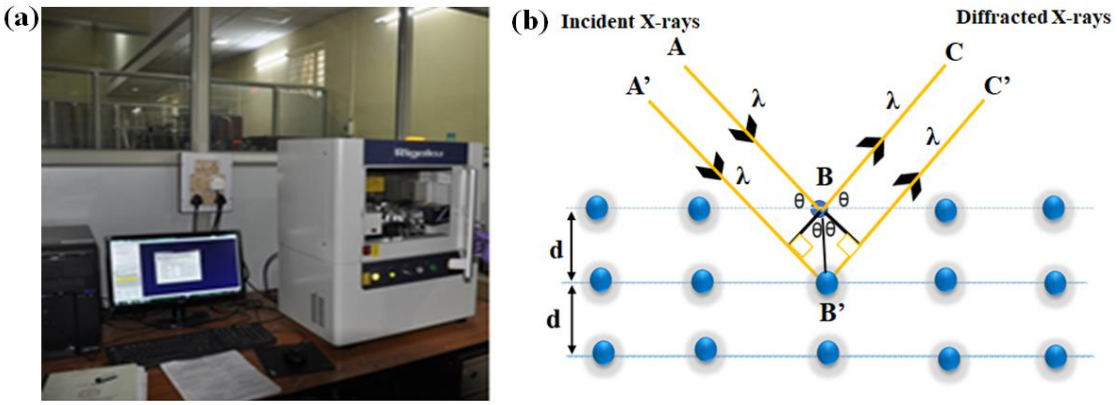

Figure 2.7 (a) Image of the Miniflex 600 X-ray Diffractometer and (b) Schematic representation of the diffraction of an X-ray beam on a crystallographic material.

2.2.2 Morphological Analysis: Scanning Electron Microscopy (SEM) and Field – emission Scanning Electron Microscopy (FE-SEM)

Scanning electron microscope (SEM) and Field–emission Scanning Electron Microscopy (FE-SEM) are both versatile instruments to get knowledge about surface topography as well as composition through the magnified images of an object.

They both fall within the category of electron microscopes that produce enlarged images of a sample by scanning their surfaces with a focused of an electron beam. SEM provides the structural information up to 200 kX magnification, a scale of up to 0.1µm (100 nm) at an accelerating voltage of up to 20.0 kV. Whereas, FE-SEM gives information about the surface features at a higher resolution and broader energy range. It works at a very low value of potential (0.02-5.0 kV) which helps to lower the damage of non-conductive specimens by charging and uses an in-lens detector which produces high-resolution images at a very low accelerating voltage. Figure 2.8 shows the FE-SEM instrument

utilized in our work is FEI NOVA NANO SEM 450 model, USA. The field emission gun is utilised in FE-SEM to generate extremely focused high and low-energy electron beams.

Figure 2.8 Photograph of the FE-SEM instrument.

The underlying idea behind both techniques is the same. In a raster scan pattern, an electron beam is scanned over the sample, interacting with the atoms in the material and produces a number of signals. A two-dimensional image that foretells the surface structure, composition and material orientation of the sample is produced after data is collected in a selected area of the sample.

A column structure of SEM as shown in Figure 2.9 (a) includes the following major components:

1. Electron Guns

2. Electron lenses (condenser and objective)
3. Apertures
4. Scanning coils
5. Detectors

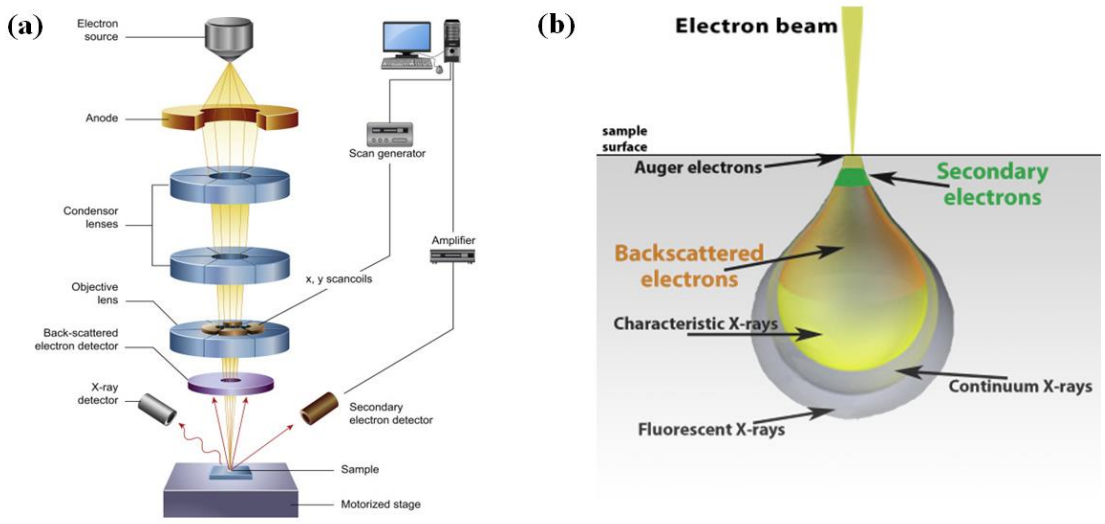

Figure 2.9 (a) Basic components of SEM (courtesy: Encyclopedia Britannica) and (b) demonstration of the several signals generated by the electron beam sample interaction.

A heated tungsten filament or single crystals of Lanthanum Hexa Boride (LaB_6) are used to produce electrons, which are then accelerated by a voltage that is typically between 20 V and 30 kV and directed down the centre of an electron optical column made up of various magnetic lenses to generate a focused stream of electrons that strikes the surface of the specimen. Scanning coils, which are located above the objective lens and enable the electron beam to be scanned over the sample surface, is used to regulate the electron beam's position on the sample. As illustrated in Figure 2.9(b) there are two types of interactions between the electron beam and the sample: inelastic interactions (Secondary electrons, SEs) and elastic interactions (Backscattered electrons, BSEs). Signals from these interactions are acquired to create the image [115,116]. SEs originate from surface regions whereas BSEs are produced from deeper areas of the sample which provides both

topographic and compositional information. As a result, it provides information on topographic contrast in an area that is suitable for visualising surface texture and the roughness. The majority of nanomaterials (conductive nature) can be loaded on carbon tape and directly viewed by SEM. Metal coating (Gold, Siver, Platinum etc.) is required for non-conductive samples (Bioorganic nanomaterials).

2.2.3 Elemental Analysis

2.2.3.1 X-ray Photoelectron Spectroscopy (XPS)

Electron Spectroscopy for Chemical Analysis (ESCA) for XPS is another name for XPS. It is the extensively applied practice to analyse the chemical state of an element and composition of the material. This technique work on the principle of photoelectric effect and the result arises in the form of the binding energy of the elements. The sample's surface can be analysed either in line-profile or in-depth profile, with the average depth of analysis~5 nm over the surface (typically occurs in conjunction with ion-beam etching) [115, 116].

In XPS, Mono-energetic Al kα x-rays excite the sample surface and emit photoelectrons from the sample surface. Then the kinetic energy of these emitted photoelectrons ($E_{kinetic}$) is measured with the help of an electron energy analyser and the binding energy of these emitted photoelectrons ($E_{Binding}$) is determined using the photoelectric effect Eq. 2.2.

$$KE_{e^-} = E_{photon} - \varphi \qquad \text{(Eq. 2.2)}$$

Where, KE_{e^-} is the kinetic energy of electron, E_{phton} is the energy of photon and φ is the binding energy.

By using an ultra-high vacuum (UHV) of $10^{-6\ to\text{-}7}$, all elements except helium and hydrogen can be identified using this technique. The chemical processes in this technique.

The chemical processes in the materials can also be examined in their as-received state as well as after cleavage, scraping, exposure to heat, reactive gasses or solutions, ultraviolet light, or during ion implantation. It gives a spectrum of Binding energy (eV) vs. the intensity of a photoelectron peak (count/sec) and obtained data is standardized at 284.4 eV (binding energy of sp^3 Carbon) by default. The wide scan XPS spectrum usually from 0 to 1200 eV is known as the Survey spectrum. The, elemental identity, , and quantity of a detected can be determined from The XPS data can be used to determine element's binding energy, elemental identification, chemical state, and amount.

Figure 2.10 Image of the XPS instrument.

2.2.3.2 Energy dispersive X-ray spectroscopy (EDX)

It is a supporting technique attached to the SEM, FE-SEM and TEM to find out the elements and their relative percentage into the specimen, giving both qualitative and quantitative analysis. The spectra show elements with relative peak intensity and also the elemental mapping of each individual element.

2.2.4 Surface Area Analysis: Brunauer-Emmett-Teller (BET) Theory

BET theory is given by Stephen Brunauer, Paul Hugh Emmett, and Edward Teller in 1938 for multilayer adsorption. It is an absorption analysis technique in which gas molecules are physically adsorbed on the solid surface and using this tool specific surface area of solid materials can be measured [117]. This theory is applicable for the system of multilayer absorption systems in which adsorbate (probing gas) are N_2, Ar, CO_2 that do not react with the adsorbent molecules. In these adsorbates, N_2 is the most frequently used adsorbate for surface area analysis therefore, measurement in BET is lead at the boiling temperature of N_2 (77 K).

The choice of the adsorbate gas is made when measuring surface area based on estimated surface area and sample properties. Assuming a monomolecular layer of the known gas, adsorbate gas is measured using a volumetric or continuous flow approach. Then, using the Rouquerol transform, the BET surface area is assessed in the linear section of the BET plot.

Prior to measurement, the sample must be properly preconditioned to eliminate physically bonded contaminants from the powder's surface. The process of is called Degassing, also known as outgassing, is a preconditioned procedure in which the sample is exposed to a high temperature (depending on its thermal properties) together with a vacuum or constantly flowing inert gas.

The BET theory is the extension of Langmuir's Theory of monolayer adsorption for multilayer adsorption. The BET equation used for specific surface area calculation from N_2 adsorption-desorption isotherm is given as follows:

$$\frac{P}{V(P^0-P)} = \frac{1}{V_m C} + \frac{C-1}{V_m C}\left(\frac{P}{P_0}\right) \qquad \text{(Eq. 2.3)}$$

Where, 'P' and 'P^0' are equilibrium and saturation vapour pressure of adsorbate at adsorption temperature T respectively, 'V_m' is the volume for monolayer adsorption and 'C' is the BET constant, which should be positive. The plot of relative pressure ($\frac{P}{P_0}$) on the x-axis and 1/V[(P^0/P)-1] on the y-axis is called a BET plot. Then, the slope and y-intercept are calculated by drawing a linear relationship in the relative pressure area of 0.05 to 0.35 and further, using the slope and y-intercept, BET constant (C) and monolayer adsorption volume (V_m) can be determined, hence the total and specific surface area are measured. Pore size distribution and pore volume distribution are examined trough BJH plot. Figure 2.11 shows the image of BET instrument and its schematic representation.

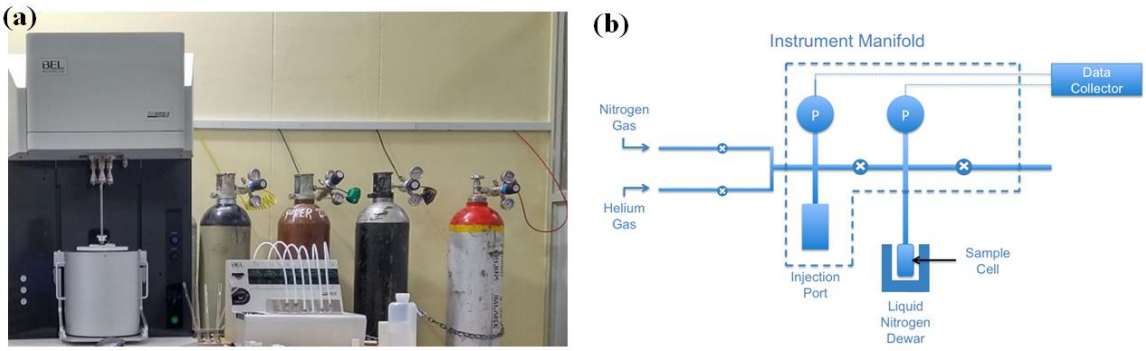

Figure 2.11 (a) Photograph of the BET instrument and (b) its schematic representation [111].

2.2.5 Thermal Analysis: Thermo gravimetric measurement (TGA)

Thermogravimetric analysis is an analytical method that controls a material's thermal stability. In this technique, weight of a sample changes over time by degradation of volatile components as the temperature increases. It generates the characteristic decomposition patterns which depict the physical as well as the chemical aspect of the sample. The phase change, adsorption-desorption, thermal breakdown and solid-gas reactions (e.g., oxidation or reduction) all are depicted on TGA graph. For the

investigation of a wide range of materials, including polymeric materials, inorganic materials, organic-inorganic hybrid materials etc., it is a highly helpful technique.

Figure 2.12 shows the TGA measurement and its block diagram of thermo-balance. It continuously measures mass while gradually changing a sample's temperature at N_2 atmosphere. It has an internal furnace with a programmable control temperature of a sample, a precision balance with a sample pan, and the temperature is raised steadily to maintain a thermal reaction. Depending on the requirements, the thermal reaction may take place in a high vacuum, high pressures, constant pressure or controlled pressure environment or in a atmosphere of ambient air.

On the y axis of the TGA curve, mass or percentage of original mass are plotted against either time temperature or on the x-axis. The differential thermal analysis and detailed interpretations can both benefit from the first derivative of the TGA curve, known as the DTG curve.

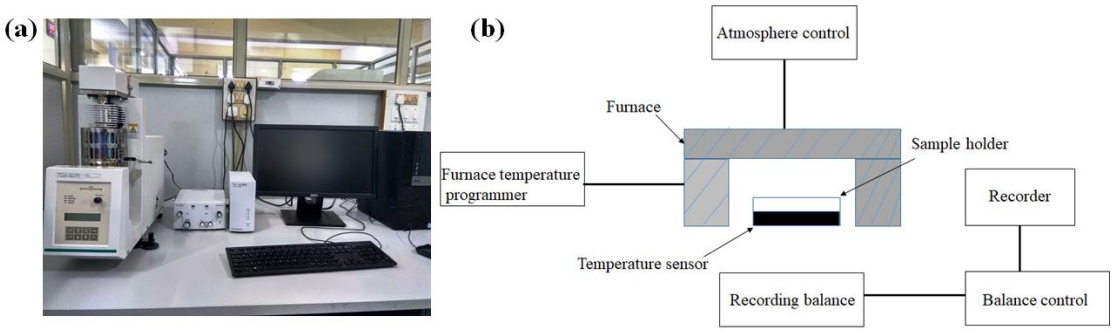

Figure 2.12 (a) Image of the TGA instrument and (b) block diagram of its thermo-balance.

2.2.6 Electrochemical measurements

This segment describes the electrochemical workstation, its components and the measurement methods to evaluate the OER performance. We used, potentiostat galvanostat (PGSTAT) Auto lab Metrohm, Nova 1.11 software for all the electrochemical measurements as shown in Figure 2.13 (a). It measures the current between the counter

and the working electrode with respect to the potential in a potentiostat mode. All the electrochemical measurements like CV (Cyclic voltammetry), LSV (linear sweep voltammetry), EIS (electrochemical impedance spectroscopy) and CA (chronoamperometry) are performed in the electrochemical cell using reference, counter and the working electrode using this instrument. We used Ag/AgCl as a reference electrode, Platinum (Pt) disc or Pt coil as a counter and glassy carbon electrode, GCE (geometric area = 0.07 cm^2) as working electrode. Herein, the RHE (reversible hydrogen electrode) scale is used for the electrode's potential presentation using the calibration Eq. 2.4.

$$E_{RHE} = E_{Ag/AgCl} + 0.059.pH + E^0_{Ag/AgCl} \qquad \text{(Eq. 2.4)}$$

$$E^0_{Ag/AgCl} = 0.210\ V$$

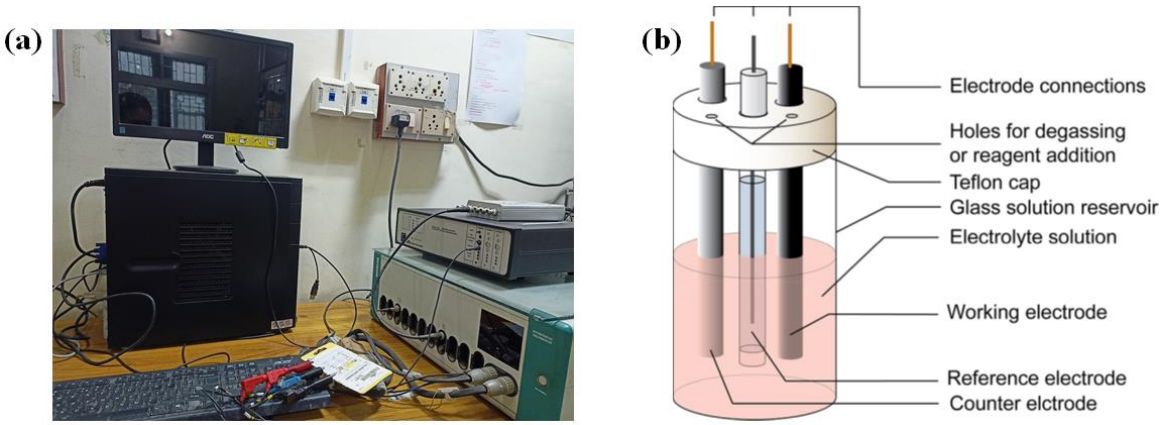

Figure 2.13 (a) Image of the Autolab NOVA instrument and (b) electrochemical cell setup [118].

2.2.6.1 Cyclic Voltammetry (CV) and Linear Sweep Voltammetry (LSV)

Cyclic voltammetry is a common and popular measurement tool to examine the redox activity of any materials. It is a potentiodynamic measurement in which the potential of the working electrode linearly varies with time at a constant scan rate gives the current as output. It is called cyclic voltammetry because it forms a cyclic waveform as the applied potential after reaching its final input value, returns back to its initial input value, giving

the output current in the cyclic form. Figure 2.14 shows the typical CV graph in which the oxidation peak is related to the upper half (positive current) and the reduction peak belongs to the lower half (negative current). It is also an important technique for investigating electron-transfer-initiated chemical reactions in catalysis.

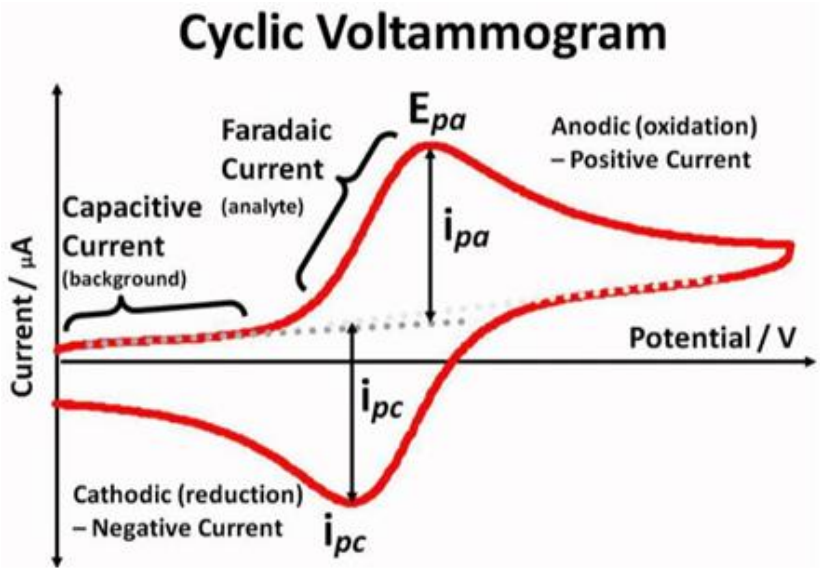

Figure 2.14 Figure of cyclic voltammogram (courtesy: Wikimedia commons).

Indeed, linear sweep voltammetry is a half cycle of the CV. It goes only in one direction and does not make a complete cycle. In LSV, a fixed potential range is applied between the working and reference electrode and the potential is linearly scanned from a lower limit to an upper with time at a fixed scan rate, measuring the output current. It gives either an oxidation or reduction peak depending on the nature of the materials and potential window. It is widely used for HER, OER and ORR measurements.

In the experiment, the scan rate governs the speed of the applied potential. The applied potential scanned slowly at a low scan rate and fast scanned at a high scan rate. Accordingly, the peak current (i_p) also depends on the scan rate as described by the well-known Randles-Sevcik equation as follows-

$$i_p = 0.4463\, nFAC\left(\frac{nF\upsilon D}{RT}\right)^{1/2} \qquad \text{(Eq. 2.5)}$$

Where $'i_p'$ is peak current, 'n' is the number of electron transfers in the redox process, 'F' is the Faraday constant, 'A' is the geometric area of the electrode, 'C' is the concentration, 'υ' is the scan rate, 'D' is the diffusion coefficient, 'R' is the gas constant and 'T' is the temperature in kelvin. From the equation, it is obvious that the peak current is directly proportional to the square root of the scan rate, as the scan rate increases, accordingly the peak current also increases (see Figure 2.15).

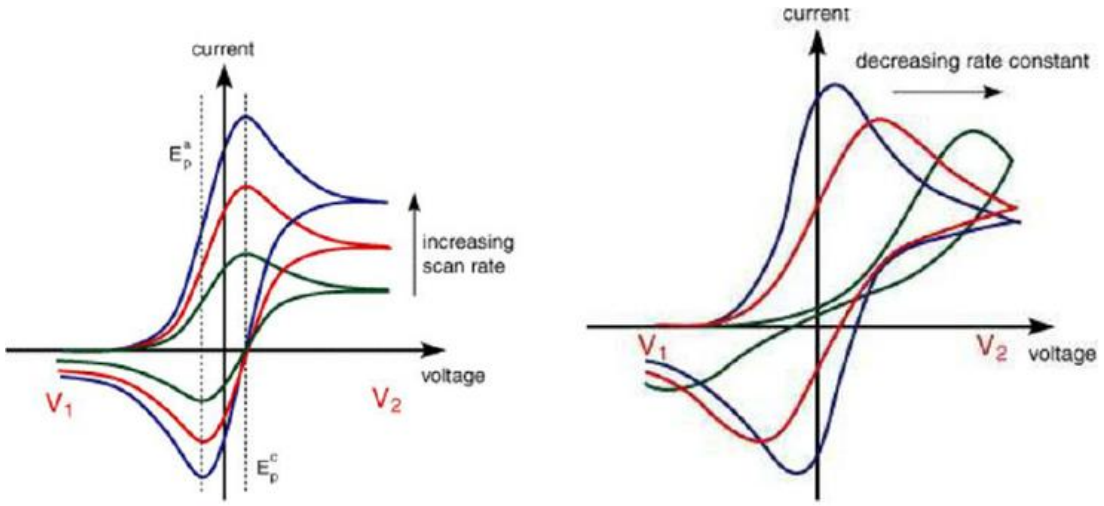

Figure 2.15 Effect of the scan rate on peak current [119].

2.2.6.2 Electrochemical Impedance Spectroscopy (EIS)

EIS is a very dynamic and well-known experimental technique to characterize the behaviour of electrochemical systems [112]. It is used for the investigation of the interfacial properties occurring at the electrode surface. Frequency of the AC source is applied in the range of 10^5 to 0.01 Hz and impedance is measured in the form of Nyquist plot (Figure 2.16) in which impedance of the electrode is recorded with respect to the frequency. In the Nyquist plot impedance at the x-axis is called 'Z_{real}' and at y-axis, it is denoted as 'Z_{img}'. There are various parameters are generated at the electrode-electrolyte

interface viz. solution resistance (R_s), charge transfer resistance (R_{ct}), capacitance and mass transfer resistance [112]. In Figure 2.16, the Nyquist plot contains two regions: the region at the high-frequency side in which a semi-circle appeared and a straight line appearing at the low-frequency region. A semi-circle is produced due to the charge transfer resistance (R_{ct}), showing the faradic process, along with the uncompensated solution resistance and straight-line presents the mass transfer impedance, known as Warburg impedance (W).

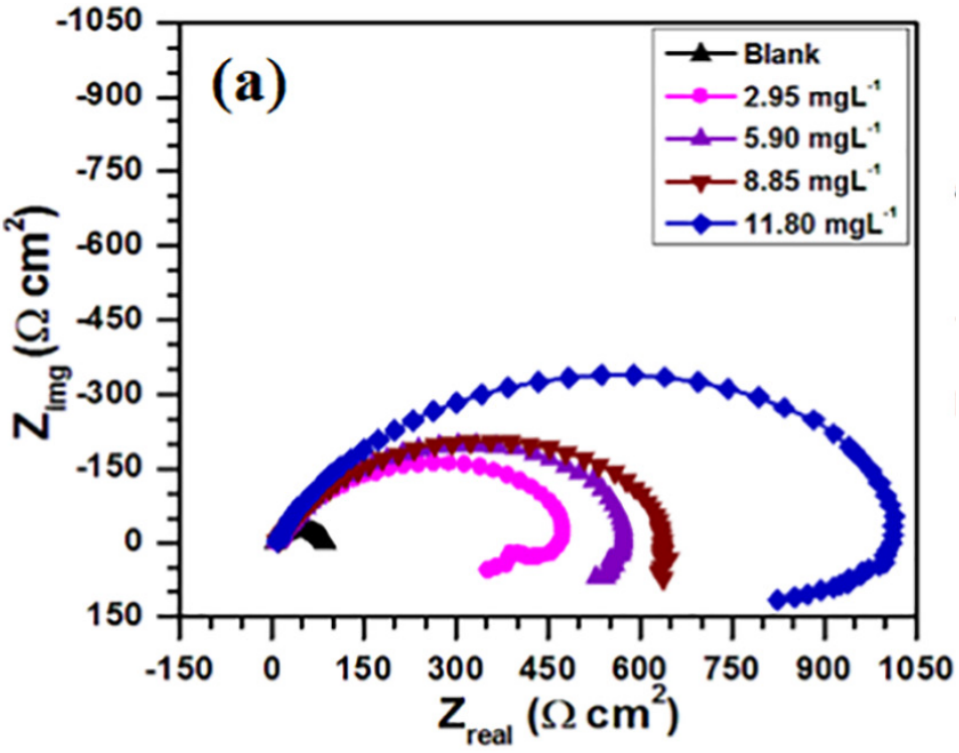

Figure 2.16 Impedance curve and its equivalent circuit [120].

2.2.6.3 Chronoamperometry (CA)

The chronoamperometry method is employed to examine the stability of the catalyst material. In this method, a fixed value of the potential is put and the current response is measured due to the faradic process. It gives the current-time graph of the diffusion-controlled process taking place at the electrode surface. A constant value of the current for a long duration implies better stability of the catalyst.

2.3 Characterisations of commercially available RuO_2

The OER performance of the above synthesised catalyst materials are compared to RuO_2. RuO_2 is used as a benchmarking catalyst for the OER reaction. XRD, SEM and BET measurements are done to investigate the crystallite size of particles, morphology and surface area.

The average crystallite size for RuO_2 is found to be ~22.6 nm (calculated using the Debye-Scherrer formula [12], $D = \frac{0.89\lambda}{\beta Cos\theta}$, (Eq. 2.6) β represents the integrated peak-width at half maxima). BET surface area is found to 8.26 m^2g^{-1}.

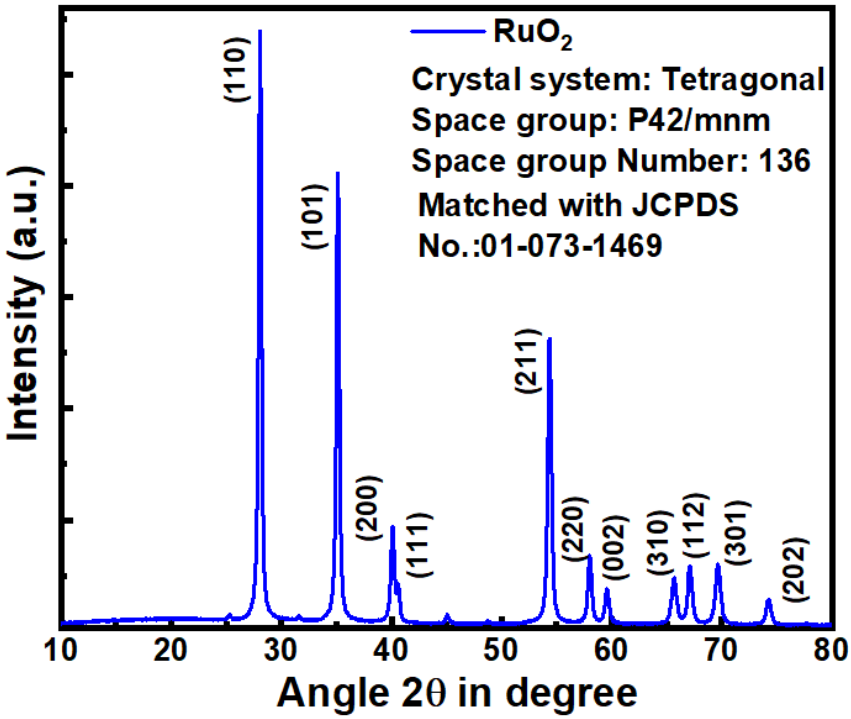

Figure 2.17 XRD pattern of commercial RuO_2.

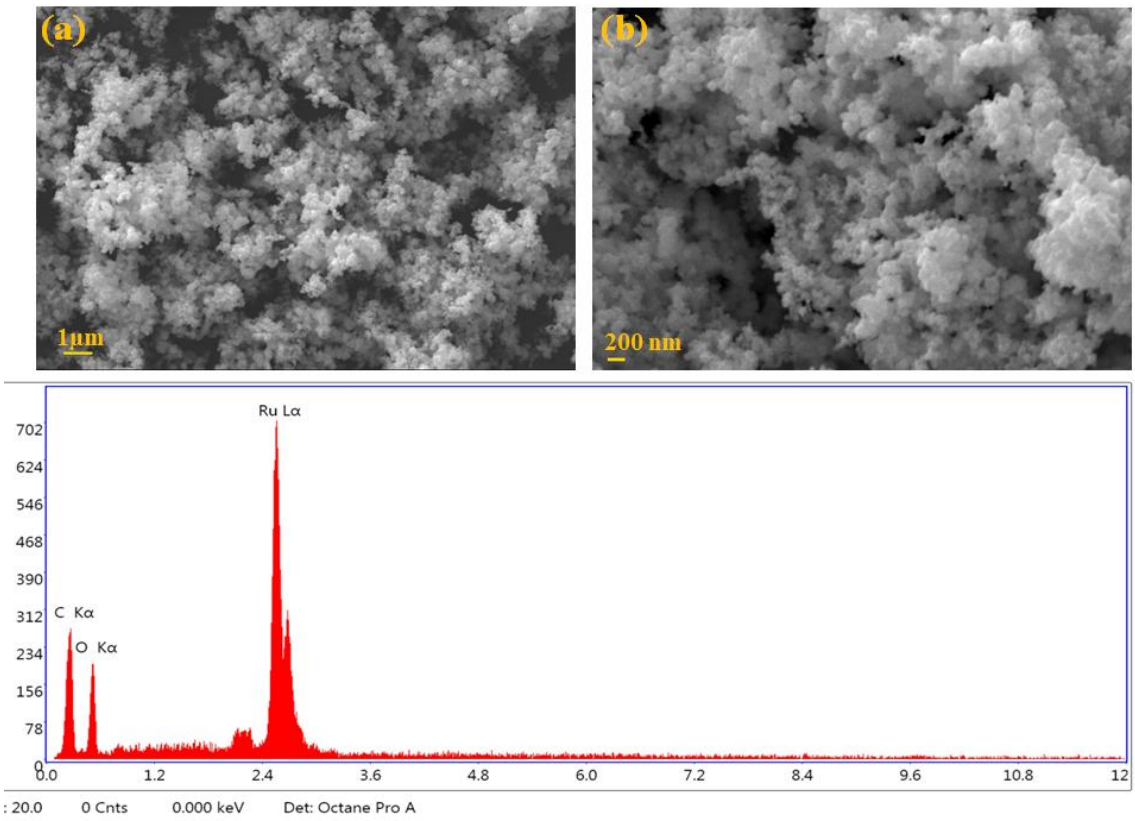

Figure 2.18 SEM images of RuO_2 at (a) 1µm, (b) 200 nm and (c) EDX (carbon present due to the coating).

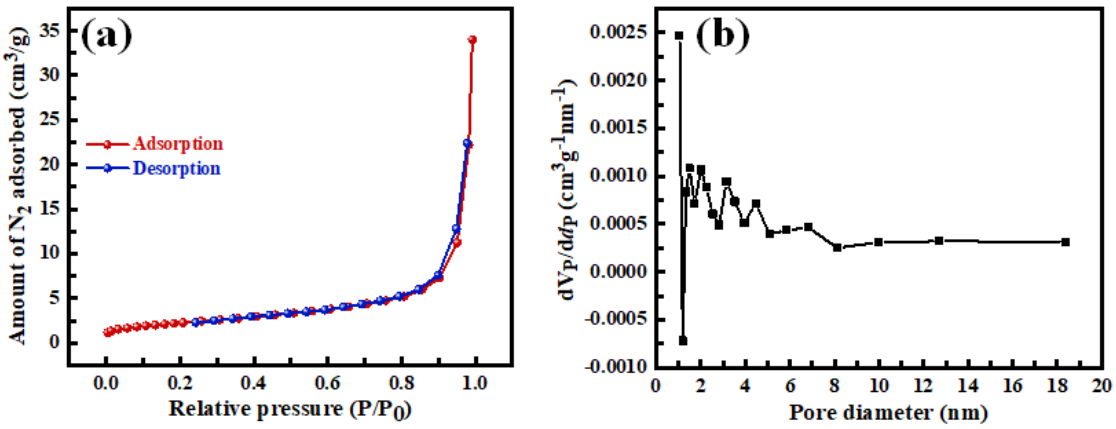

Figure 2.19 (a) N_2 adsorption-desorption isotherm and (b) pore area distribution plot of RuO_2.